Am J Transl Res 2019;11(12):7324-7337
www.ajtr.org /ISSN:1943-8141/AJTR0101965

Original Article

Transplanted mouse liver stem cells at different stages of differentiation ameliorate concanavalin A-induced acute liver injury by modulating Tregs and Th17 cells in mice

Shanshan Li[1,2*], Yanzhen Bi[1,2*], Quanquan Wang[3], Manman Xu[1,2], Zhenglai Ma[1,2], Yonghong Yang[4], Yongkai Chang[5], Suling Chen[6], Derong Liu[7], Zhongping Duan[1,2], Feng Hong[4], Yu Chen[1,2]

[1]Difficult and Complicated Liver Diseases and Artificial Liver Center, Beijing Youan Hospital, Capital Medical University, Beijing 100069, China; [2]Beijing Municipal Key Laboratory of Liver Failure and Artificial Liver Treatment Research, Beijing 100069, China; [3]Department of Neuromuscular Disease, The Third Hospital of Hebei Medical University, Shijiazhuang 050000, Hebei, China; [4]Institute of Liver Diseases, Affiliated Hospital of Jining Medical University, Jining 272000, Shandong, China; [5]Department of Neurosurgery, Fuxing Hospital, Capital Medical University, Beijing 100038, China; [6]Department of Infectious Disease, Heping Hospital Affiliated to Changzhi Medical College, Changzhi 046000, Shanxi, China; [7]Elyon Biotechnologies, Gaithersburg, MD 20879, USA. [*]Equal contributors.

Received September 5, 2019; Accepted December 1, 2019; Epub December 15, 2019; Published December 30, 2019

Abstract: Acute liver failure (ALF) is a disease with a considerably high mortality rate that still lacks a safe and effective treatment. Transplantation of liver stem cells (LSCs) has been considered to be a promising therapeutic alternative for ALF since LSCs have been shown to be involved in immunomodulation and functional reconstruction of the liver. Our present study evaluated and compared the protective effects of the two mouse LSC lines, YE and R5, as well as those of adult mouse hepatocyte (HC), on concanavalin A (ConA)-induced acute liver injury. YE and R5 cells were analyzed by microscopy, functional assays, and gene expression. We confirmed that YE and R5 cells were undifferentiated cells that had partial hepatocytic functions and a potential to differentiate into hepatocytes. YE cells has characteristics of LSCs at the early stage of differentiation, whereas the differentiation stage of R5 cells was later than that of YE cells. Subsequently, YE, R5, and HC cells were intraperitoneally transplanted into three groups of mice, followed by injection of ConA through the tail vein of each mouse at 12 h later. Blood tests, histology, flow cytometry, and quantitative PCR were then used to evaluate the therapeutic effects of the cell transplantations at 24 h after ConA injections. Compared with that of the ConA control group, YE, R5, and HC cells reduced the expression of alanine transaminase (ALT), aspartate aminotransferase (AST), and total bilirubin (TBIL) in serum and alleviated the degree of hepatic necrosis. Moreover, transplantation of these cells induced more regulatory T cells (Tregs) and less T-helper 17 (Th17) cells in the liver and spleen, and also promoted the expression of forkhead box protein 3 (Foxp3) and interleukin (IL)-10; in contrast, these transplantations induced various degrees of inhibition in the expression of retinoic acid-related orphan receptor γt (RORγt), IL-17A, IL-17F, and tumor necrosis factor-α (TNF-α). The protective effects of YE and R5 cells were significantly stronger than those of HC cells, and YE cells at the earlier differentiation stage than that of R5 cells exhibited the strongest protective effects. These results demonstrate that mouse LSCs at different stages of differentiation alleviate ConA-induced acute liver injury in mice by modulating Tregs, Th17 cells, and cytokine secretion.

Keywords: Acute liver failure, mouse liver stem cells, different stages of differentiation, cell transplantation, Tregs, Th17 cells

Introduction

The liver is one of the most important organs of the human body, and its functions involve energy metabolism, biological detoxification, biosynthesis, and bile secretion. Acute liver failure (ALF) is a severe condition characterized by widespread hepatocyte necrosis, acute disorder of liver function and subsequent multiorgan failure, which seriously endangers human

health [1, 2]. Concanavalin A (ConA) administration can significantly increase liver transaminase activity and inflammatory responses. The established ConA-induced acute liver injury model is characterized by hepatic necrosis, activation of T lymphocytes, and overexpression of pro-inflammatory cytokines and free radicals [3]. Therefore, this model has been used extensively to study the pathogenesis of ALF [4, 5].

Orthotopic liver transplantation is currently viewed as one of the most effective therapeutic regimens for ALF. Unfortunately, liver transplantation is limited by the shortage of donor organs, contraindications, high costs, and immunological suppression in recipients [6]. Hence, there is still an urgent need to identify and develop novel therapeutic regimens for treating ALF.

Stem cell transplantation has improved prospects for the treatment of many lethal diseases [7-11]. Liver stem cells (LSCs) are early undifferentiated cells and have the advantage of directly differentiating into hepatocytes and biliary cells. LSCs are involved in immunomodulation, proliferation, and repairment in the processes of liver diseases and are relatively ideal stem cells for the treatment of liver diseases [12-14]. We have previously isolated LSCs from adult human liver to establish a human LSC line, HYX1, that can be maintained for 50 passage and which has been successfully applied in animal experiments [5, 15]. With the continued development of improved techniques for isolating and culturing stem cells, LSCs are expected to become a novel approach for treating ALF.

Regulatory T cells (Tregs) and T-helper 17 (Th17) cells are subsets of $CD4^+$ T cells, and each are mutually restricted in terms of their differentiation and functions. Many studies have shown that these two T-cell subsets are involved in the process of liver injury [16-18]. Tregs, defined based on their expression of the transcription factor, forkhead box protein 3 (Foxp3) [19], are involved in the protection of immune-mediated liver injury through direct contact with cells or via release of anti-inflammatory cytokines, such as interleukin (IL)-10. In contrast, Th17 cells, defined based on their expression of the transcription factor, retinoic acid-related orphan receptor γt (RORγt) [20], are involved in mediating inflammatory responses and exacerbating liver injury by inducing the release of pro-inflammatory cytokines, such as IL-17 and tumor necrosis factor-alpha (TNF-α). Hence, a balance between Tregs and Th17 cells plays an important role in the pathogenesis of ALF. In our present study, we compared the protective effects and underlying mechanisms of mouse LSCs at different stages of differentiation on ConA-induced ALF. The results of this study may contribute to the development of LSCs transplantation therapy as a novel clinical treatment for ALF.

Materials and methods

Isolation of YE, R5, and HC cells

A healthy eight-week-old male C57BL/6 mouse (purchased from Beijing Weitong Lihua Company, China) was selected for the isolation of mouse LSCs. This mouse was intraperitoneally injected with 0.1 ml of 10% CCL_4 oil solution twice a week for three consecutive weeks. After the three weeks of injections, the mouse was anesthetized and perfused with 30-50 ml of ethyleneglycol-bis (2-aminoethylether)-N,N,N',N'-tetraacetic acid (EGTA) buffer and 0.05% type-IV collagenase through the portal vein for 10 min until the liver tissues became soft and showed signs of dissolution. Subsequently, the liver tissue was minced, followed by centrifuging the tissue suspension at 50×g at 4°C for 2 min. The supernatant was collected and further centrifuged at 150×g at 4°C for 8 min. The resulting pellet was resuspended in Dulbecco's modified eagle medium (DMEM; Gibco, Gran Island, NY, USA) and centrifuged at 150×g at 4°C for 5 min. Pellets containing LSCs were resuspended in phosphate-buffered saline (PBS), followed by purification in a gradient solution containing 50%, 70%, and 90% Percoll (Sigma-Aldrich), as well as the cell suspension itself. The gradient solution was prepared layer by layer by filling the highest to lowest percentages of Percoll solutions sequentially from the bottom of the tube and, lastly, adding the cell suspension on the top of the tube. The formulation was centrifuged at 350×g at 4°C for 20 min. The cell layer between the 50% and 70% Percoll solutions was transferred carefully into a new tube and centrifuged at 350×g for 5 min. The cell pellet was then resuspended in DMEM and centrifuged twice at

1,200 rpm at 4°C for 5 min. The collected LSCs were cultured in six-well plates with DMEM containing 10% fetal bovine serum (FBS; Gibo, Grand Island, NY, USA), 100 U/ml of penicillin, 100 μg/ml of streptomycin, 1 mg/l of insulin, and 1×10^{7} mol/l of dexamethasone for 2-3 weeks, with the media being changed twice a week. Once the colonies became visible, the cells were isolated using cloning cylinders and were subcultured into individual wells of a 96-well plate for further culturing. The propagated cells were harvested for the evaluation of LSC markers. Through this method, we successfully isolated two mouse LSC cell lines, named YE and R5. Coincidentally, the YE and R5 LSC lines were derived from the same mouse and had the same genetic background. The initial batches of YE and R5 cells were cultured for 20 days, and the cells were photographed after the tenth passage under a phase-contrast microscope (CKX31, Olympus, Tokyo, Japan). We were able to subculture the YE and R5 cells to more than 100 passages. In addition, we obtained hepatocytes (HCs) from an eight-week-old healthy male C57BL/6 mouse by portal vein perfusion, according to methods described in a previous study [21]. High-resolution cytology of YE, R5, and HC cells were examined via transmission electron microscopy (TEM; JEOL, Tokyo, Japan). Subsequently, the cells were transferred to T-75 culture flasks. At confluence, cells were taken for subsequent experiments.

Transmission electron microscopy (TEM)

As described above, transmission electron microscopy (TEM) was used for the morphological analysis of cells. In brief, the cells were fixed in 2.5% glutaraldehyde at 4°C for 2 h. After washing with PBS, the cells were fixed in 1% osmium tetroxide (OsO_4) for 1 h, followed by dehydration in different concentrations of ethanol (55%, 75%, and 95%) for 15 min each, absolute ethanol for 20 min, and absolute acetone for 20 min. The cells were then closed in EPON-812, followed by preparation of ultra-thin sections (120 nm in thickness). The cell sections were stained with 2% uranyl acetate for 20 min and lead citrate for 5 min before observing cytology by TEM.

Indocyanine green (ICG) uptake assays

An indocyanine green (ICG; Sigma-Aldrich, Shanghai, China) uptake assay was used to analyze the hepatic functions of YE and R5 cells. In brief, YE and R5 cells (10th passage) were treated with 1 mg/ml of ICG for 1 h at 37°C, followed by two washes in PBS, after which they were observed under a CKX31 microscope.

Periodic acid-schiff (PAS) staining

Periodic acid-schiff (PAS) staining was used to assess the glycogen storage function of the assayed cells. YE and R5 cells (10th passage) were treated with 4% paraformaldehyde solution for 10 min, followed by washing in PBS, air-drying, and subsequently treating cells with 1% periodic acid (Beijing Chemical Works, Beijing, China). The cells were then stained with PAS (Sigma-Aldrich) for 30 min at room temperature, followed by three washes in PBS, and were subsequently observed under a CKX31 microscope.

Detection of urea and albumin (ALB) content in the culture supernatants of YE, R5, and HC cells

YE, R5, and HC cells were seeded at a density of 5×10^{5} cells per well in six-well plates and were cultured for 24 h, 36 h, and 48 h, followed by collection of their supernatants to detect urea and albumin (ALB) levels via an automated analyzer (AU5800, Beckman Coulter, Brea, CA).

Reverse transcription-polymerase chain reaction (RT-PCR) for YE and R5 cells

The mRNA levels expression of *ALB*, alpha fetoprotein (*AFP*), cytokeratin *CK-8*, *CK-18,* and *CK-19* in YE and R5 cells were measured by reverse transcription-polymerase chain reaction (RT-PCR). Total RNA from YE and R5 cells was extracted using a RNAiso kit (Takara, Otsu, Japan). Moloney murine leukemia virus reverse transcriptase (M-MLV) was used for cDNA synthesis, followed by use of these cDNAs as templates for PCR. The PCR products were separated by electrophoresis, and the separated DNA bands in the gels were photographed. The corresponding primer sequences are listed in **Table 1**. The original RT-PCR image was shown in Figure S1.

Mice and treatments

In this study, male C57BL/6 mice weighing 22-25 g (purchased from Beijing Weitong Lihua

Table 1. RT-PCR primer sequences

Target gene	Forward primer	Reverse primer
ALB	5'-TCGCTACACCCAGAAAGCAC-3'	5'-CACACACGGTTCAGGATTGC-3'
AFP	5'-TGCGTGACGGAGAAGAATGT-3'	5'-AACACCCATCGCCAGAGTTT-3'
CK8	5'-CGGGGGATCCAACACTTTCA-3'	5'-CAGCTTCCCATCTCGGGTTT-3'
CK18	5'-CACCAACATCACAAGGCTGC-3'	5'-TGAGATTTGGGGGCATCCAC-3'
CK19	5'-GGGGGTTCAGTACGCATTGG-3'	5'-GAGGACGAGGTCACGAAGC-3'

Company, China) were maintained according to the guidelines of the National Institutes of Health, and all procedures were approved approved by the Institutional Animal Care and Use Committee of Jining Medical University Affiliated Hospital. The mice were housed at the Animal Care Facility of Jining Medical University with a 12-h light-dark cycle at a constant temperature. All mice had free access to tap water throughout the study. Forty male C57BL/6 mice were randomly divided into the following five groups (n = 8): normal control (normal); ConA control (ConA); and three cell-intervention groups, including YE, R5, and HC groups. Mice in the normal group were intraperitoneally injected with the same amount of PBS, followed by injection of PBS via the tail vein at 12 h later. Mice in the ConA group were intraperitoneally injected with the same amount of PBS, followed by injection of 12 mg/kg of ConA via the tail vein at 12 h later. Mice in the three cell-intervention groups were intraperitoneally transplanted with 2×10^6 YE, R5, and HC cells per animal, followed by injection of ConA via the tail vein at 12 h later. Mice in the ConA and the three cell-intervention groups were euthanized at 24 h after the ConA injection. The mice in the normal group were euthanized at 24 h after the final PBS injection. The blood serum of all mice in the different groups were collected for the detection of biochemical parameters. Liver tissues were collected for histopathological examinations and detection of inflammatory cytokines. Flow cytometry was used to detect the levels of Tregs and Th17 cells in liver and spleen tissues.

Blood serum analysis

Blood samples were collected from the orbital plexus of each animal before euthanization, followed by centrifugation at 3,000 rpm for 15 min to collect serum. The levels of alanine transaminase (ALT), aspartate aminotransferase (AST), and total bilirubin (TBIL) were measured by an automatic analyzer (AU5800, Beckman Coulter, Brea, CA).

Flow cytometry analysis

The liver and spleen tissues of each mouse were homogenized to collect the constituent cells, which were washed twice with PBS containing 1% FBS and 1% NaN_3. Subsequently, the cells were incubated with anti-CD4, anti-CD25, anti-IL-17, and anti-Foxp3 primary antibodies at 4°C for 30 min according to standard procedures. After two washes with PBS, the cells were analyzed using a FACSCalibur flow cytometer (Becton Dickinson, San Jose, CA, USA). An isotype control was used for each antibody during flow cytometry.

Hematoxylin and eosin staining

Liver tissues at the same location as that used for flow cytometry samples were collected, followed by rinsing with PBS, fixing in 4% formalin, and paraffin-embedding. The samples were then sectioned and stained with hematoxylin and eosin dye (H&E).

Quantitative PCR (qPCR) analysis of mouse liver samples

Total RNA was extracted from 30 mg of mouse liver tissue, followed by using RNA (5 μg) for the reverse transcription into cDNA. The SYBR green quantitative PCR (qPCR) Master Mix (Annoron, Roche, Beijing, China) was used for qPCR in a LightCycler® 480 Real-Time PCR System (Annoron, Roche, Beijing, China). Analysis was performed in triplicate for qPCR. The corresponding primer sequences for qPCR used in this study are listed in **Table 2**.

Statistical analysis

All results are presented as the mean ± standard error of the mean (SEM). SPSS 22.0 software (IBM, Armonk, NY, USA) was used for statistical analysis. The differences among groups were compared by one-way analysis of variance (ANOVA), followed by pairwise comparisons via Bonferroni *post-hoc* tests. $^*P < 0.05$ and $^{**}P < 0.01$ were considered statistically significant.

Table 2. Quantitative PCR primer sequences

Target gene	Sequence (5'-3')	Product (bp)
GAPDH	F: GGCAAATTCAACGGCACAGT	111
	R: GGCCTCACCCCATTTGATGT	
IL-10	F: TCAAGGCGCATGTGAACTCC	176
	R: GATGTCAAACTCACTCATGGCT	
IL-17A	F: AGCGTGTCCAAACACTGAGG	160
	R: ATCAGGGTCTTCATTGCGGT	
IL-17F	F: CTTGCAGAAGGCTGGGAACT	151
	R: GGGGTCTCGAGTGATGTTGT	
TNF-α	F: CCCTCACACTCAGATCATCTTCT	61
	R: GCTACGACGTGGGCTACAG	
Foxp3	F: CTGGGGAAGCCATGGCAATA	181
	R: GGCGAACATGCGAGTAAACC	
RORγt	F: GTGGGGACAAGTCATCTGGG	103
	R: GTGCAGGAGTAGGCCACATT	

Results

Morphological characterization of YE, R5, and HC cells

During culturing, the rapidly proliferating YE cells attached to the culture plate and appeared as small and round or oval-shaped (**Figure 1A**). The volumes of R5 cells were slightly larger than those of YE cells, adhered to the culture plate more easily, and resembled mature hepatocytes (**Figure 1B**). In subsequent subcultures, both YE and R5 cells appeared in larger and flatter shapes that were more similar to those of mature hepatocytes. The volumes of the mature HC cells were significantly larger than those of YE and R5 cells, and exhibited as polyhedral shapes (**Figure 1C**). The HC cells adhered to the culture plate at 8 h after being isolated from the liver. TEM showed that most of the YE and R5 cell bodies were occupied by their oval nuclei, and the ratio of the nucleus-to-cytoplasm was large. The main organelles, such as mitochondria and ribosomes, were underdeveloped, resembling the characteristics of undifferentiated cells (**Figure 1D** and **1E**). The nucleus-to-cytoplasm ratios of mature HC cells were smaller than those of YE and R5 cells, with the nucleus of each cell exhibiting as a round shape located at the center, and containing one to two nucleoli. Some nuclei were binuclear. The cytoplasms of mature HC cells were filled with developed organelles, such as mitochondria, endoplasmic reticuli, and ribosomes (**Figure 1F**).

Functional characterization of YE, R5, and HC cells

An ICG uptake assay showed that both YE and R5 cells were able to uptake ICG, with cells exhibiting a pale-green color (**Figure 1G** and **1H**). PAS staining showed a large number of positive cells stained in red (**Figure 1I** and **1J**). These results indicated that YE and R5 cells had partial functions of hepatocytes. Subsequently, we used RT-PCR to evaluate the mRNA levels of hepatocyte and biliary epithelial cell markers in YE and R5 cells. The results showed that both YE and R5 cells expressed the hepatocyte marker genes, *ALB, CK8,* and *CK18*, as well as the biliary epithelial cell marker gene, *CK19* (**Figure 1K**). In addition, we observed YE, R5, and HC cells for 48 h and compared their abilities to synthesize urea and ALB in the 24 h, 36 h, and 48 h cultures. The levels of urea in the culture supernatants of YE and R5 cells were higher than those in the control (Blank), but were lower than those in HC cells at 24 h, 36 h, and 48 h. The urea synthesis of the R5 cells was stronger than that of the YE cells at 24 h and 36 h (**Figure 2A**). The levels of ALB in the culture supernatants of YE and R5 cells were not higher than those of the blank at 24 h or 36 h. The levels of ALB in the culture supernatants of YE and R5 cells were higher than those of the blank and lower than those of the HC cells at 48 h. The ALB synthesis of the R5 cells was stronger than that of the YE cells at 48 h (**Figure 2B**). In total, the synthetic functions of urea and ALB in YE and R5 cells were weaker than those of HC cells, and the urea and ALB synthesis of the R5 line was stronger than that of the YE line, suggesting that the R5 cell line was relatively similar to mature HC cells in terms of synthetic function.

Biochemical analysis after the transplantation of YE, R5, and HC cells

To evaluate the effects of the three cells in alleviating ConA-induced acute liver injury, we compared serum ALT, AST, and TBIL levels in the different groups of mice and found that the serum ATL and AST levels in the ConA group were significantly higher than those in the normal group, while they were decreased in the YE, R5, and HC groups. The serum TBIL levels in the ConA group were significantly higher than those in the normal group, while they were decreased in the YE and R5 groups. The serum ASL and TBIL levels in the YE group were lower

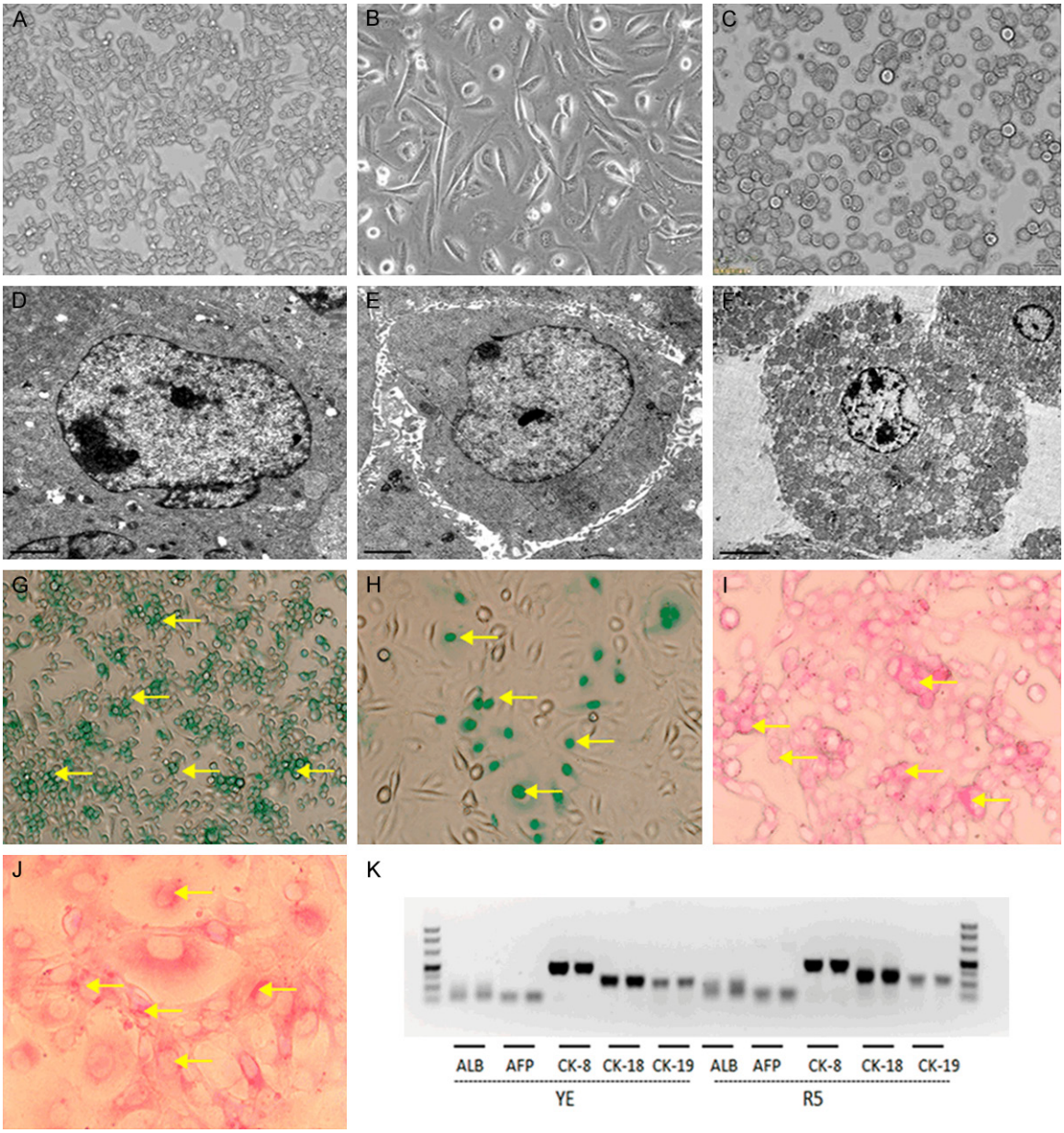

Figure 1. Characteristics of cellular morphology of YE, R5, and HC cells. Functional analysis and expressions of marker genes in YE and R5 cells. Representative images under light microscopy (original magnification ×200) of YE cells (A), R5 cells (B), and mature HC cells (C); Representative TEM images of a YE cell (D), R5 cell (E), and HC (F); ICG uptake assay showing pale-green ICG-positive YE cells (G) and R5 cells (H) (as indicated by the yellow arrows). PAS staining of YE cells (I) and R5 cells (J) showing positive cells with cytoplasm appeared red (as indicated by the yellow arrows). (K) RT-PCR showing that YE and R5 cells expressed both hepatocyte marker genes-*ALB, CK8,* and *CK18*-and the biliary epithelial cell marker gene, *CK19*.

than those in the R5 group (**Figure 3**). Overall, the protective effects of YE and R5 cells were significantly stronger than those of the HC cells, and YE cells had the best protective effect among the three cells. These results suggest that intraperitoneal transplantation of LSCs induces a protective effect in ConA-induced acute liver injury.

Histopathology after the transplantation of YE, R5, and HC cells

Obvious hyperemic and swollen livers with a large number of bleeding spots and congestion were observed visually in the ConA group. These conditions were alleviated in the YE, R5, and HC groups, wherein the YE group demon-

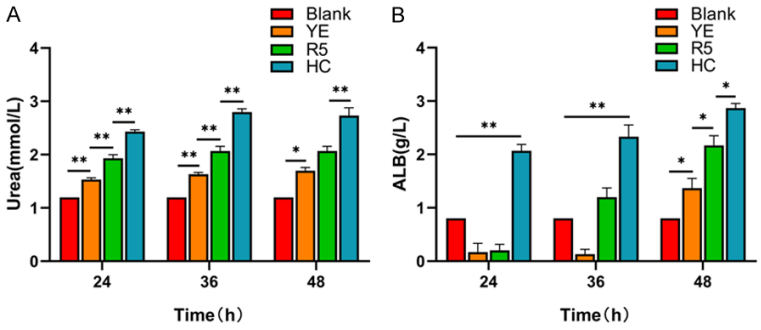

Figure 2. Both YE and R5 cells synthesized urea and ALB, but their functions of synthesizing urea and ALB were weaker than those of HC cells. Synthesis levels of urea (A) and albumin (ALB) (B) in the culture supernatants of YE, R5, and HC cells were detected by an automatic analyzer when cultured for 24 h, 36 h, and 48 h. Data are presented as the mean ± SEM (n = 3; $^{*}P < 0.05$, $^{**}P < 0.01$).

strated the most obvious alleviation (**Figure 4A**). Morphological analysis via H&E staining under light microscopy (**Figure 4B** and **4C**) showed no obvious cell degeneration or necrosis in the liver tissues of the normal group. In contrast, hepatocellular congestion and oedema were obvious in the ConA group, with massive inflammatory cells infiltration in the liver parenchyma and bile ducts, destruction of the hepatic lobule structure, and extensive necrotic areas; these pathologies that were indicative of liver tissue injury were all ameliorated in the YE, R5, and HC groups. Only a small amount of inflammatory cell infiltration was found in the liver tissues of the YE group, with only rare punctate necrosis and laminar necrosis. The liver tissues of the R5 group had scattered bridging necrosis and focal necrosis. The liver tissues of the HC group had obvious liver cell congestion and oedema, as well as partial punctate necrosis and laminar necrosis. The necrosis area of eight random, nonoverlapping fields was quantitatively measured in liver tissues of ConA-induced ALF mice from different experimental groups. The liver necrosis in the ConA group was the most serious, while such necrosis was ameliorated in the YE, R5, and HC groups. The areas of liver necrosis in the YE and R5 groups were less than those in the HC group, among them, the area of liver necrosis in the YE group was the least (**Figure 4D**). These changes were consistent with differences observed in the biochemical data, suggesting that intraperitoneal transplantation of YE, R5, and HC cells had protective effects on ConA-induced acute liver injury. Among them, YE and R5 cells exhibited stronger protective effects than those of HC cells, and YE cells demonstrated the best protective effects.

Modulation of Tregs and Th17 cells after transplantation of YE, R5, and HC cells

The balance of Tregs and Th17 cells controls the development of autoimmunity and inflammation and has been considered to be a potential therapeutic target for liver injury. For these reasons, the present study analyzed the effects of intraperitoneal transplantation of YE, R5, and HC cells on the proportions of Tregs and Th17 cells in the liver and spleen of the ConA-induced ALF mouse model. The proportions of Tregs and Th17 cells in the liver and spleen were significantly increased after ConA injection. Compared with that in the ConA group, intraperitoneal transplantation of YE, R5, and HC cells significantly upregulated the proportion of Tregs in the liver and spleen (**Figure 5A** and **5B**) and also suppressed the upregulation of the proportion of Th17 cells (**Figure 5C** and **5D**). Overall, intraperitoneal transplantation of YE, R5, and HC cells regulated the Treg/Th17 cell balance with varying degrees in the context of ConA-induced liver injury. Among them, YE and R5 cells exhibited significantly stronger regulation than that of HC cells, and YE cells demonstrated the best overall regulation.

Detection of IL-10, IL-17A, IL-17F, TNF-α, Foxp3, and RORγt mRNA levels in liver via qPCR after transplantation of YE, R5, and HC cells

The immune functions of cytokines secreted by Tregs and Th17 cells are quite different from one another. Tregs secrete IL-10, which has an immunosuppressive effect. Th17 cells mainly secrete IL-17 (IL-17A and IL-17F) and TNF-α, which induce inflammation and promote immune-mediated liver injury. Based on these differences, we measured mRNA levels of IL-10, IL-17A, IL-17F, and TNF-α in the livers of each group and found similar results to the above findings based on flow cytometry. The IL-10

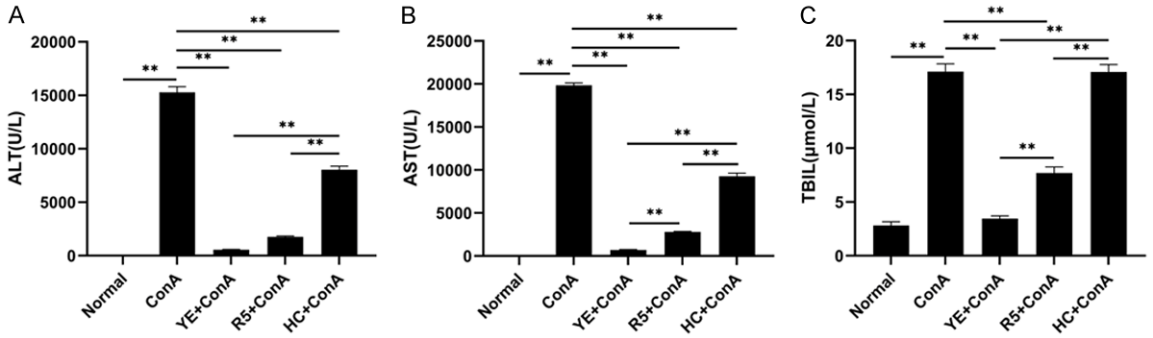

Figure 3. YE, R5, and HC cells ameliorated the liver functions in ConA-induced ALF mice. The protective effects of YE and R5 cells were significantly stronger than those of the HC cells, and YE cells had the best protective effect among the three cells. Some liver functional parameters including ATL (A), AST (B), and TBIL (C) were determined in Normal, ConA, YE, R5, and HC group mice. Data are presented as the mean ± SEM (n = 8; $^{*}P < 0.05$, $^{**}P < 0.01$).

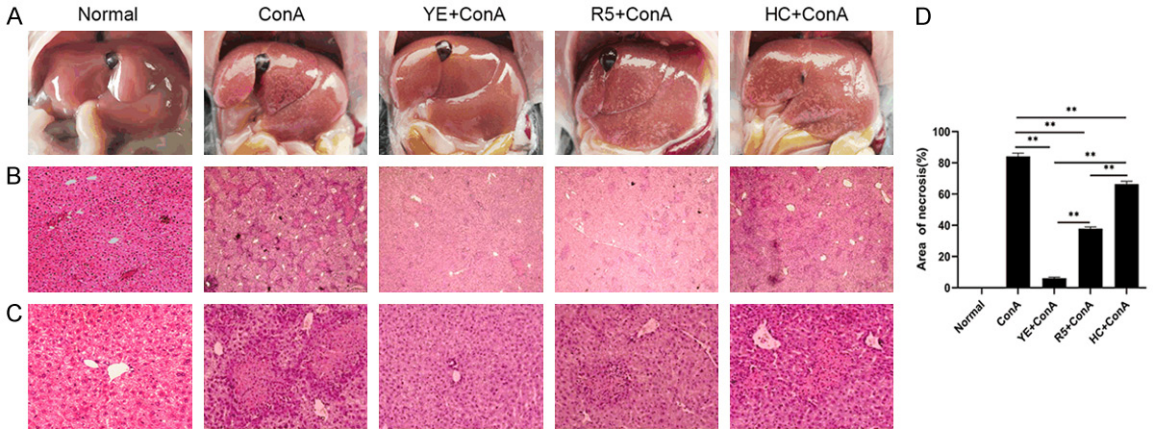

Figure 4. YE, R5, and HC cells ameliorated the hepatic damage in ConA-induced ALF mice. The YE cells had the best protective effect among the three cells. (A) Visual observation of livers in Normal, ConA, YE, R5, and HC groups of mice. (B, C) Representative images of hematoxylin and eosin staining of liver tissues in the five groups of mice with original magnifications of ×40 (B) and ×200 (C). (D) Measurements of necrosis area. Bar chart comparing the quantification of necrosis areas in the liver tissues in the five groups of mice. Data are presented as the mean ± SEM (n = 8; $^{*}P < 0.05$, $^{**}P < 0.01$).

mRNA levels in the liver of the ConA group were significantly higher than those in the normal group. Intraperitoneal transplantation of YE and R5 cells significantly enhanced the above upregulation of IL-10 mRNA. In contrast, intraperitoneal transplantation of HC cells did not enhance the above upregulation of IL-10 mRNA (**Figure 6A**). The mRNA levels of IL-17A, IL-17F, and TNF-α in the liver of the ConA group were significantly higher than those of the normal control group. Intraperitoneal transplantation of YE and R5 cells suppressed the upregulation of IL-17A, IL-17F, and TNF-α mRNA. In contrast, intraperitoneal transplantation of HC cells only suppressed the upregulation of IL-17A mRNA (**Figure 6B-D**). These results indicate that YE and R5 cells enhanced the ConA-induced upregulation of the anti-inflammatory cytokine, IL-10, and suppressed the upregulation of the pro-inflammatory cytokines-IL-17A, IL-17F, and TNF-α-in the liver. In contrast, HC cells only suppressed the ConA-induced upregulation of IL-17A in the liver.

To further explore how YE and R5 cells regulated the Treg/Th17 ratio in the ConA-induced ALF mouse model, we measured mRNA levels of key transcription factors of Treg and Th17 cells, Foxp3 and RORγt, respectively, in the livers of the different groups. The mRNA levels of RORγt in the livers of the ConA group were significantly upregulated compared to those in the normal

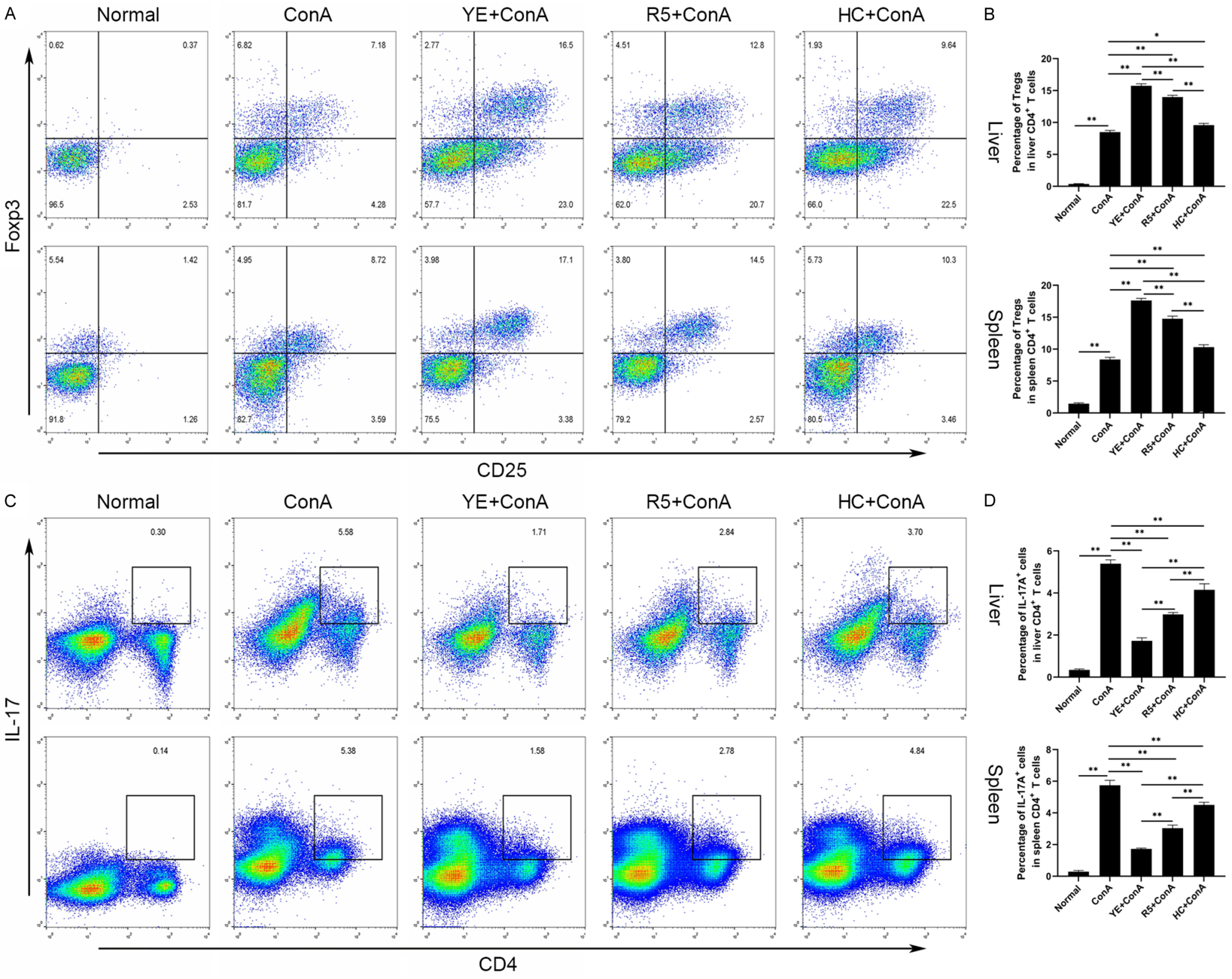
A
Normal
ConA
YE+ConA
R5+ConA
HC+ConA
Foxp3
CD25
0.62
0.37
96.5
2.53
6.82
7.18
81.7
4.28
2.77
16.5
57.7
23.0
4.51
12.8
62.0
20.7
1.93
9.64
66.0
22.5
5.54
1.42
91.8
1.26
4.95
8.72
82.7
3.59
3.98
17.1
75.5
3.38
3.80
14.5
79.2
2.57
5.73
10.3
80.5
3.46
B
Liver
Spleen
Percentage of Tregs in liver CD4+ T cells
Percentage of Tregs in spleen CD4+ T cells
Normal
ConA
YE+ConA
R5+ConA
HC+ConA
C
IL-17
CD4
0.30
5.58
1.71
2.84
3.70
0.14
5.38
1.58
2.78
4.84
D
Percentage of IL-17A+ cells in liver CD4+ T cells
Percentage of IL-17A+ cells in spleen CD4+ T cells

Figure 5. YE, R5, and HC cells regulated the Treg/Th17 cell balance in ConA-induced ALF mice. YE and R5 cells exhibited stronger regulation than that of HC cells, and YE cells demonstrated the strongest regulation. A. Density plots of flow cytometry results of $CD4^+/CD25^+/Foxp3^+$ Tregs in the livers and spleens in Normal, ConA, YE, R5, and HC groups of mice. B. Bar charts comparing the percentages of Tregs in the livers and spleens. C. Density plots of flow cytometry results of $CD4^+/IL\text{-}17A^+$ Th17 cells in livers and spleens in the five groups of mice. D. Bar charts comparing the percentages of Th17 cells in the livers and spleens. Data are presented as the mean ± SEM (n = 8; $^*P < 0.05$, $^{**}P < 0.01$).

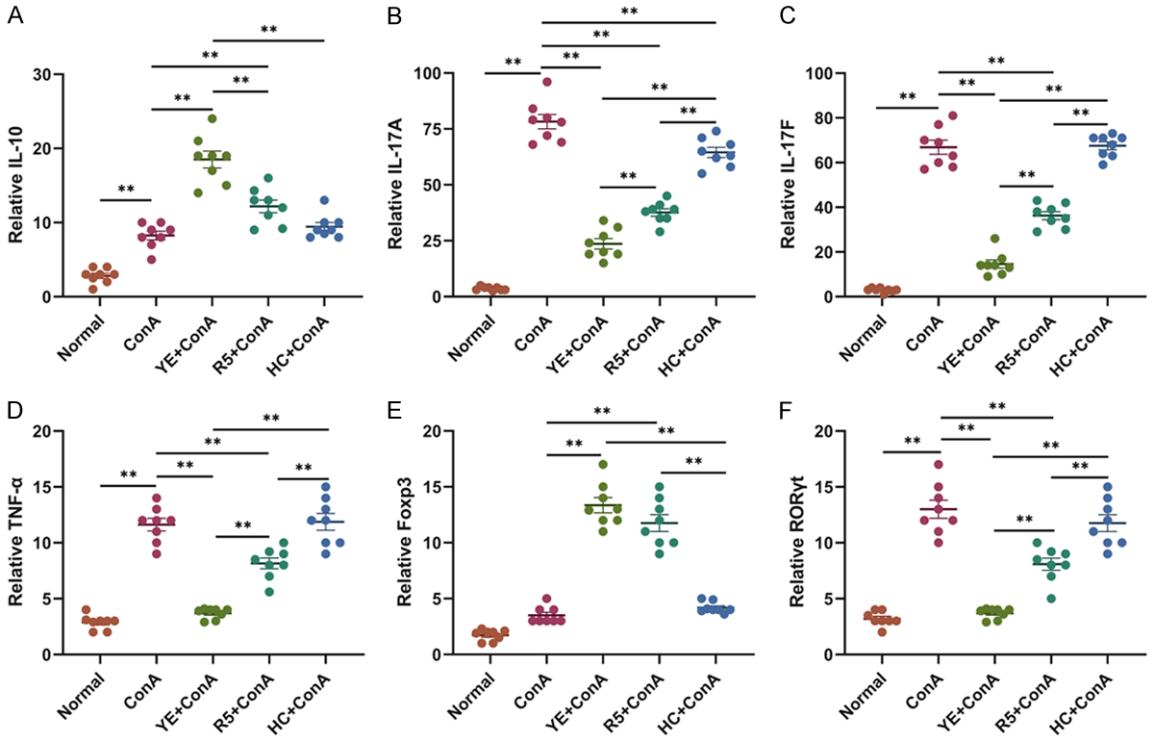

Figure 6. YE, R5, and HC cells regulated the mRNA levels of cytokines-IL-10, IL-17A, IL-17F, and TNF-α-and transcription factors-Foxp3, and RORγ-in ConA-induced ALF mice. The regulatory effects of YE and R5 cells were significantly stronger than those of HC cells, with YE cells exhibiting the most optimal regulation. Quantitative PCR (qPCR) was used to detect the mRNA levels of IL-10 (A), IL-17A (B), IL-17F (C), TNF-α (D), Foxp3 (E), and RORγt (F) in the livers of Normal, ConA, YE, R5, and HC groups of mice. Data are presented as the mean ± SEM (n = 8; $^*P < 0.05$, $^{**}P < 0.01$).

control group. The intraperitoneal transplantation of YE and R5 cells upregulated Foxp3 mRNA and suppressed the upregulation of RORγt mRNA in the liver after the ConA injection. In contrast, intraperitoneal transplantation of HC cells failed to modulate the expression of Foxp3 and RORγt mRNA (**Figure 6E** and **6F**). These results indicate that intraperitoneal transplantation of YE, R5, and HC cells ameliorated ConA-induced liver injury through regulating Tregs and Th17 cells and their related cytokines. Overall, the regulatory effects of YE and R5 cells were significantly stronger than those of HC cells, with YE cells exhibiting the most optimal regulation.

Discussion

ALF is a serious life-threatening disease, with liver transplantation representing the only effective therapeutic strategy. However, the scarcity of matched liver sources, high costs, and life-long immunosuppression have hampered the development of liver transplantations. In our study, we used a ConA-induce ALF mouse model, which is one of the most commonly used models for studying immune liver injury, mainly through activating $CD4^+$ T cells and natural-killer T cells to induce specific liver damage. However, the optimal doses for modeling ALF are varied in different reports. In the early stage of our experiments, we found that

the appropriate ConA dose for modeling ALF was 12 mg/kg, which resulted in serious liver injury in mice, yet no mice died within 24 h after the ConA injection. Hence, the modeling effect with the use of 12 mg/kg ALF was stable and sufficient. Therefore, a series of experimental studies were conducted using this specific ConA dose [5, 22]. In addition, we selected the optimal time point of cell intervention based on the results of a previous study in our laboratory. Guided by the results of our previous study, we employed an intraperitoneal transplantation of cells at 12 h before the ConA injection and evaluated the effects of stem cell intervention at 24 h post-ConA injection, when the most severe hepatic inflammatory response is known to occur [5].

Numerous studies have used hepatocytes to treat liver disease, which has achieved specific therapeutic effects [23, 24]. However, many problems-such as the limited number of hepatocytes, inability to expand hepatocytes *in vitro*, uncertain quality of donor hepatocytes, and possible rejection after the transplantation-limit the application of hepatocytes in the treatment of ALF. Given the remarkable characteristics of self-proliferation, low rejection, and bidirectional differentiation into hepatocytes or biliary epithelial cells, LSCs provide a new direction for the treatment of liver failure and have aroused considerable attention in recent years. Our research team successfully developed the human LSC line, HYX1. In the present study we also developed two mouse LSC lines, YE and R5, from the same mouse liver. These two cell lines have been subcultured for more than 100 passages, and have been successfully applied in animal experiments.

Our study identified and compared the morphological and functional characteristics of YE, R5, and HC cells via light microscopy, electron microscopy, ICG uptake, PSA staining, the measurement of urea and ALB synthesis, and gene expression. The results of light and electron microscopy suggested that, compared with those of HC cells, YE and R5 cells had characteristics of undifferentiated cells, including small cell bodies, large nuclei, less cytoplasmic space, and underdeveloped organelles. ICG is a water-soluble anionic complex that is only taken up and excreted by hepatocytes. Hence, ICG is commonly used to assess the functions of hepatocytes [25]. Glycogen synthesis and storage by hepatocytes are also important functions in vivo. Positive PAS staining represents another marker of hepatocyte function. In the present study, both YE and R5 cells uptook and excreted ICG, and were stained by PAS. Urea is a substance synthesized only by hepatocytes. In the present study, both YE and R5 cells synthesized urea and ALB. However, since both YE and R5 cells were both still in the undifferentiated stage, their functions of synthesizing urea and ALB were weaker than those of HC cells. Results of RT-PCR in our present study showed that YE and R5 cells expressed markers of both hepatocyte and biliary epithelial cell. These results indicated that YE and R5 cells were still in an undifferentiated stage and had some functions of hepatocytes and potential to differentiate into hepatocytes. In addition, we focused on comparing some of the characteristics of YE and R5 cells and showed that the cell volumes of R5 cells were larger than those of YE cells. R5 cells had similar growth habits to those of HepG2 cells and mature hepatocytes in the culture and they were more likely to adhere to the wall, with their morphology close to that of mature HC cells after adherence, compared with that of the YE line. In terms of the syntheses of urea and ALB, R5 cells were more similar to mature HC cells. These characteristics suggested that the differentiation stage of the R5 line was later than that of the YE line.

In the ConA-induced ALF mouse model, biochemical analysis and H&E staining showed that intraperitoneal transplantation of YE, R5, and HC cells reduced serum ALT, AST, and TBIL levels and alleviated hepatic necrosis. Our results were similar to the findings of Nagamoto et al. [26], which prepared human induced pluripotent-stem-cell-derived hepatocyte-like cells (iPS-HLCs) into cell sheets and adhered the cell sheets to the liver surfaces of mice with ALF induced by carbon tetrachloride. This cell sheet secreted hepatocyte growth factor to protect the liver. To date, more and more studies have shown that implanted stem cells inhibit the secretion of inflammatory mediators, regulate immune responses, and inhibit fatal cytokine cascades via paracrine secretion, thereby alleviating liver damage in ALF [14, 27, 28]. In the present study, the protective effects of YE and R5 cells on liver injury were more pronounced

than those of HC cells, suggesting that LSCs have stronger paracrine and immunomodulatory functions than those of mature HC cells during ALF.

To further investigate the underlying mechanisms of YE and R5 cells in alleviating ConA-induced ALF, we examined the levels of Tregs and Th17 cells in the livers and spleens of each group of mice. T cells play a key role in the pathogeneses of many liver diseases; for example, Tregs inhibit innate and adaptive immune responses and exert suppressive effects on T cell-mediated inflammation in the course of disease. In contrast, Th17 cells mediate inflammatory responses and promote the development of immune-mediated liver injury by producing cytokines, such as IL-17A, IL-17F, and TNF-α. Increasing evidence indicates that the balance between Tregs and Th17 cells is critical to maintain immune hemostasis in many liver diseases, and a disruption of this balance may lead to severe liver damage [16-18, 29]. In the present study, intraperitoneal transplantation of YE and R5 cells enhanced Tregs upregulation and suppressed Th17 cells upregulation in the livers and spleens of the ConA-induced ALF mouse model, suggesting that YE and R5 cells ameliorated ConA-induced liver injury in mice through regulating the balance between Tregs and Th17 cells. In addition, detection of cytokine levels in the liver tissues showed that YE and R5 cells exerted protective effects by upregulating the anti-inflammatory cytokine IL-10 and by downregulating pro-inflammatory cytokines-such as IL-17A, IL-17F, and TNF-α. Further experiments showed that YE and R5 cells upregulated the expression of the Tregs transcription factor Foxp3, and downregulated the expression of the Th17 transcription factor RORγt. Overall, among the different cells tested, our findings suggest that LSC YE cells in the earlier stage of differentiation exerted the most powerful regulation and protection in ConA-induced ALF.

In summary, we isolated two LSC lines (YE and R5) at different stages of differentiation from the adult mouse liver, and characterized their stem cellular phenotypes. Our present study demonstrated the efficacy of LSCs in the amelioration of ConA-induced acute liver injury by regulating the balance of Tregs and Th17 cells and their cytokine secretions. Furthermore, LSCs at the earlier stage of differentiation showed stronger immunomodulatory effects and protective effect on ALF. However, the precise mechanisms of Tregs and Th17 cells in this process in terms of improving liver function need to be further clarified. In our future studies, we plan to elucidate possible mechanisms of such immunomodulation/protection via whole-genome sequencing and mass-spectrograph analysis. Collectively, our present findings provide further evidence for the use of LSCs for the treatment of ALF.

Acknowledgements

The present study was supported by funding from the Natural Science Foundation of China (No. 81170395, 81570556), National Key R&D Program of China (No. 2017YFA0103000) and National Science and Technology Key Project on "Major Infectious Diseases such as HIV/AIDS, Viral Hepatitis Preventon and Treatment" (NO. 2012ZX10002004-006, 2017ZX10203201-005, 2017ZX10201201-001-001, 2017ZX10201201-002-002, 2017ZX102022-03-006-001, 2017ZX10302201-004-002).

Disclosure of conflict of interest

None.

Address correspondence to: Yu Chen, Difficult and Complicated Liver Diseases and Artificial Liver Center, Beijing Youan Hospital, Capital Medical University, Beijing 100069, China. E-mail: chybeyond@163.com; Feng Hong, Institute of Liver Diseases, Affiliated Hospital of Jining Medical University, Jining 272000, Shandong, China. E-mail: fenghong9508@163.com

References

[1] Sass DA and Shakil AO. Fulminant hepatic failure. Liver Transpl 2005; 11: 594-605.
[2] Elias E. Liver failure and liver disease. Hepatology 2006; 43: S239-242.
[3] Heymann F, Hamesch K, Weiskirchen R and Tacke F. The concanavalin A model of acute hepatitis in mice. Lab Anim 2015; 49: 12-20.
[4] He GW, Gunther C, Kremer AE, Thonn V, Amann K, Poremba C, Neurath MF, Wirtz S and Becker C. PGAM5-mediated programmed necrosis of hepatocytes drives acute liver injury. Gut 2017; 66: 716-723.
[5] Bi Y, Li J, Yang Y, Wang Q, Wang Q, Zhang X, Dong G, Wang Y, Duan Z, Shu Z, Liu T, Chen Y,

Zhang K and Hong F. Human liver stem cells attenuate concanavalin A-induced acute liver injury by modulating myeloid-derived suppressor cells and CD4(+) T cells in mice. Stem Cell Res Ther 2019; 10: 22.

[6] Starzl TE. The long reach of liver transplantation. Nat Med 2012; 18: 1489-1492.

[7] Trounson A and McDonald C. Stem cell therapies in clinical trials: progress and challenges. Cell Stem Cell 2015; 17: 11-22.

[8] Bordignon C. Stem-cell therapies for blood diseases. Nature 2006; 441: 1100-1102.

[9] Lindvall O and Kokaia Z. Stem cells for the treatment of neurological disorders. Nature 2006; 441: 1094-1096.

[10] Lin BL, Chen JF, Qiu WH, Wang KW, Xie DY, Chen XY, Liu QL, Peng L, Li JG, Mei YY, Weng WZ, Peng YW, Cao HJ, Xie JQ, Xie SB, Xiang AP and Gao ZL. Allogeneic bone marrow-derived mesenchymal stromal cells for hepatitis B virus-related acute-on-chronic liver failure: a randomized controlled trial. Hepatology 2017; 66: 209-219.

[11] Shi M, Zhang Z, Xu R, Lin H, Fu J, Zou Z, Zhang A, Shi J, Chen L, Lv S, He W, Geng H, Jin L, Liu Z and Wang FS. Human mesenchymal stem cell transfusion is safe and improves liver function in acute-on-chronic liver failure patients. Stem Cells Transl Med 2012; 1: 725-731.

[12] Michalopoulos GK and Khan Z. Liver stem cells: experimental findings and implications for human liver disease. Gastroenterology 2015; 149: 876-882.

[13] Itoh T and Miyajima A. Liver regeneration by stem/progenitor cells. Hepatology 2014; 59: 1617-1626.

[14] Herrera MB, Fonsato V, Bruno S, Grange C, Gilbo N, Romagnoli R, Tetta C and Camussi G. Human liver stem cells improve liver injury in a model of fulminant liver failure. Hepatology 2013; 57: 311-319.

[15] Bi Y, Liu X, Si C, Hong Y, Lu Y, Gao P, Yang Y, Zhang X, Wang Y, Xiong H, Duan Z, Chen Y and Hong F. Transplanted adult human hepatic stem/progenitor cells prevent histogenesis of advanced hepatic fibrosis in mice induced by carbon tetrachloride. Am J Transl Res 2019; 11: 2350-2358.

[16] Zhang H, Jiang Z and Zhang L. Dual effect of T helper cell 17 (Th17) and regulatory T cell (treg) in liver pathological process: from occurrence to end stage of disease. Int Immunopharmacol 2019; 69: 50-59.

[17] Feng TT, Zou T, Wang X, Zhao WF and Qin AL. Clinical significance of changes in the Th17/Treg ratio in autoimmune liver disease. World J Gastroenterol 2017; 23: 3832-3838.

[18] Liang XS, Li CZ, Zhou Y, Yin W, Liu YY and Fan WH. Changes in circulating Foxp3(+) regulatory T cells and interleukin-17-producing T helper cells during HBV-related acute-on-chronic liver failure. World J Gastroenterol 2014; 20: 8558-8571.

[19] Marson A, Kretschmer K, Frampton GM, Jacobsen ES, Polansky JK, MacIsaac KD, Levine SS, Fraenkel E, von Boehmer H and Young RA. Foxp3 occupancy and regulation of key target genes during T-cell stimulation. Nature 2007; 445: 931-935.

[20] Ciofani M, Madar A, Galan C, Sellars M, Mace K, Pauli F, Agarwal A, Huang W, Parkhurst CN, Muratet M, Newberry KM, Meadows S, Greenfield A, Yang Y, Jain P, Kirigin FK, Birchmeier C, Wagner EF, Murphy KM, Myers RM, Bonneau R and Littman DR. A validated regulatory network for Th17 cell specification. Cell 2012; 151: 289-303.

[21] Li WC, Ralphs KL and Tosh D. Isolation and culture of adult mouse hepatocytes. Methods Mol Biol 2010; 633: 185-196.

[22] Bi YZ, Fan Z, Chen DF, Li SS, Wang QY, Gao PF, Wang QQ, Duan ZP, Chen Y, Kong LB, Wang YB and Hong F. Protective effect of intraperitoneal transplantation of human liver-derived stem cells at different times against concanavalin A-induced acute liver injury in mice. Zhonghua Gan Zang Bing Za Zhi 2017; 25: 205-210.

[23] Dhawan A, Puppi J, Hughes RD and Mitry RR. Human hepatocyte transplantation: current experience and future challenges. Nat Rev Gastroenterol Hepatol 2010; 7: 288-298.

[24] Pareja E, Cortes M, Bonora A, Fuset P, Orbis F, Lopez R and Mir J. New alternatives to the treatment of acute liver failure. Transplant Proc 2010; 42: 2959-2961.

[25] Liu QW, Liu QY, Li JY, Wei L, Ren KK, Zhang XC, Ding T, Xiao L, Zhang WJ, Wu HY and Xin HB. Therapeutic efficiency of human amniotic epithelial stem cell-derived functional hepatocyte-like cells in mice with acute hepatic failure. Stem Cell Res Ther 2018; 9: 321.

[26] Nagamoto Y, Takayama K, Ohashi K, Okamoto R, Sakurai F, Tachibana M, Kawabata K and Mizuguchi H. Transplantation of a human iPSC-derived hepatocyte sheet increases survival in mice with acute liver failure. J Hepatol 2016; 64: 1068-1075.

[27] Ratajczak MZ, Kucia M, Jadczyk T, Greco NJ, Wojakowski W, Tendera M and Ratajczak J. Pivotal role of paracrine effects in stem cell therapies in regenerative medicine: can we translate stem cell-secreted paracrine factors and microvesicles into better therapeutic strategies? Leukemia 2012; 26: 1166-1173.

[28] Shi D, Zhang J, Zhou Q, Xin J, Jiang J, Jiang L, Wu T, Li J, Ding W, Li J, Sun S, Li J, Zhou N, Zhang L, Jin L, Hao S, Chen P, Cao H, Li M, Li L, Chen X and Li J. Quantitative evaluation of human bone mesenchymal stem cells rescuing fulminant hepatic failure in pigs. Gut 2017; 66: 955-964.

[29] Xu L, Gong Y, Wang B, Shi K, Hou Y, Wang L, Lin Z, Han Y, Lu L, Chen D, Lin X, Zeng Q, Feng W and Chen Y. Randomized trial of autologous bone marrow mesenchymal stem cells transplantation for hepatitis B virus cirrhosis: regulation of Treg/Th17 cells. J Gastroenterol Hepatol 2014; 29: 1620-1628.

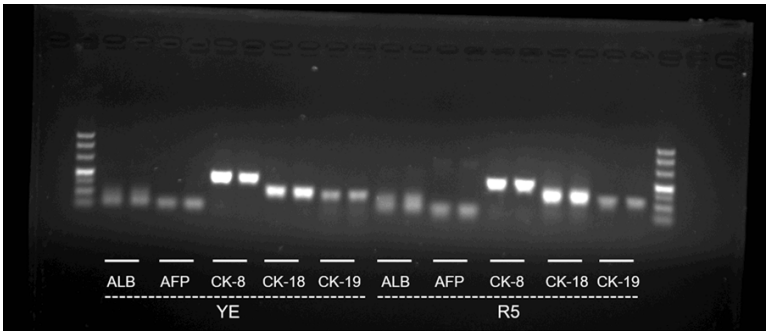

Figure S1. The original RT-PCR image for **Figure 1K**.